SUPPLEMENTARY INFORMATION

SqueeSAR™ and GPS Ground Deformation Monitoring of Santorini Volcano (1992-2012): Tectonic Implications

By

Lagios[1] E., Sakkas[1] V., Novali[2] F., Bellotti[2] F., Ferretti[2] A., Vlachou[1] K. & Dietrich[3] V.

(1) Remote Sensing Laboratory, Geophysics-Geothermics Dept., University of Athens, Panepistimiopolis-Ilissia, Athens 157 84, Greece.

(2) Tele-Rilevamento Europa T.R.E. s.r.l., Ripa di Porta Ticinese 79, Milano 21149, Italy.

(3) Institute for Geochemistry and Petrology, Swiss Federal Institute of Technology, CH-8092 Zurich, Switzerland

Contents

1. Inferred Faults from Geophysical Analysis 2

2. Comparing GPS and SqueeSAR (Period 1992 – 2010) 6

3. Strain Field Deduced by GPS Measurements (*Unrest* Period) 7

4. Mogi Model Parameter Estimates by various Authors 8

5. Estimated CGPS Velocities for Distinct Periods 9

6. PS/DS Time Series for selected points in Nea Kammeni & Therassia for the Period 1992-2010 11

7. PS/DS Time Series for selected points in Kammenis & Imerovigli for the Period 2011-2012 12

1. Inferred Faults from Geophysical Analysis

A new Gravity Anomaly Map of Santorini (Fig. 1) was recently homogenized and compiled by Chailas et al. (2012) using more than 550 gravity measurements from various sources (Yokoyama and Bonasia, 1971; 1979; Budetta et al., 1984; Vassiliadis, 1985; Lagios, 1995; National Geophysical Data Center (USA), 2012). A focus on the southern part of Thera is presented in this section with emphasis on the investigation of faults without a surface trace, and the possible basement extent at the south-eastern part.

It is qualitatively clear from this map that the Alpine basement outcrop at the southern part of Thera, extending to the Monolithos area to the north, is associated with the gravity high where the anomaly values are higher than about 130 mGal. The gravity low (110 mGal) identified around the Akrotiri area is due to the low density overburden (eg. tuffs) and the partially met Akrotiri lavas. Results of a 3-D gravity inversion modeling that was performed at an attempt to investigate the subsurface basement variations and possible faults, together with the thickness of the pyroclastics, were also taken into consideration in this paper (after Chailas et al., 2012) at an attempt to model hidden faults. Data from the two boreholes S2 and S3 (Fytikas et al., 1989) along Profile AB (Fig. 1) were used to constrain the modeling. A density contrast of 1.7 Kg/m^3 was chosen based on laboratory measurements on basement samples from the southern area of Santorini, and published work (Budetta et al., 1984; Boyce and Gertisser, 2012). Two possible basement faults (running almost N-S and presented in Fig. 1) are interpreted along Profile AB, one between S2 and S3 boreholes, and another one about 2 km west of borehole S2, marking a depression (the Akrotiri Depression) in the broader area of Akrotiri.

The location of these two faulting features is in agreement with earlier Audio-Magnetotelluric work carried out in that region for the exploration of its geothermal potential. Figure 2b shows the polarization ellipse of the maximum electric field and the real vectors averaged over the frequency interval 0.5 Hz to 0.01 Hz, which corresponds to relatively deep parts of the geoelectric structure (2 – 5 km).

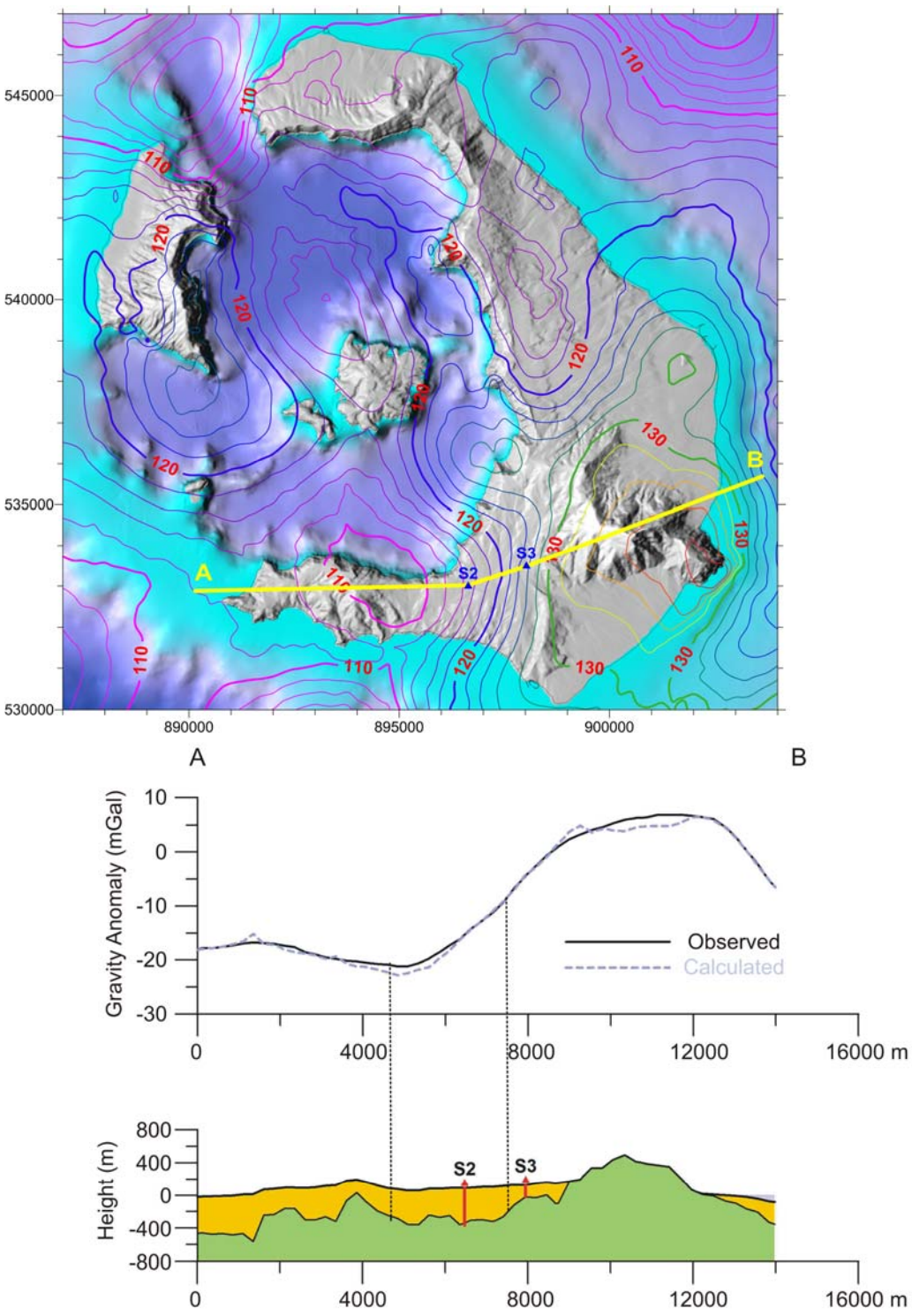

Figure 1. Santorini Gravity Anomaly Map referred to IGSN'71 and GRF'67 Contour interval 2 mGal; AB: Gravity Profile along which the basement variation is shown deduced from a 3-D gravity inversion modeling. Two boreholes (marked as S2 and S3) were used for modeling control (after Chailas et al., 2012).

The overall configuration of the electric field and current flow indicates that the deeper structure is simpler and smoother than the shallower structure (Fig. 2a). Only one large scale structural trend (striking N320°-330°) is detected and comprises a relatively broad elongated conductor extending between the Akrotiri Peninsula and the Kammenis. These two faults seem to play an important role in the kinematics of the southern part of Thera greatly controlling the observed deformation.

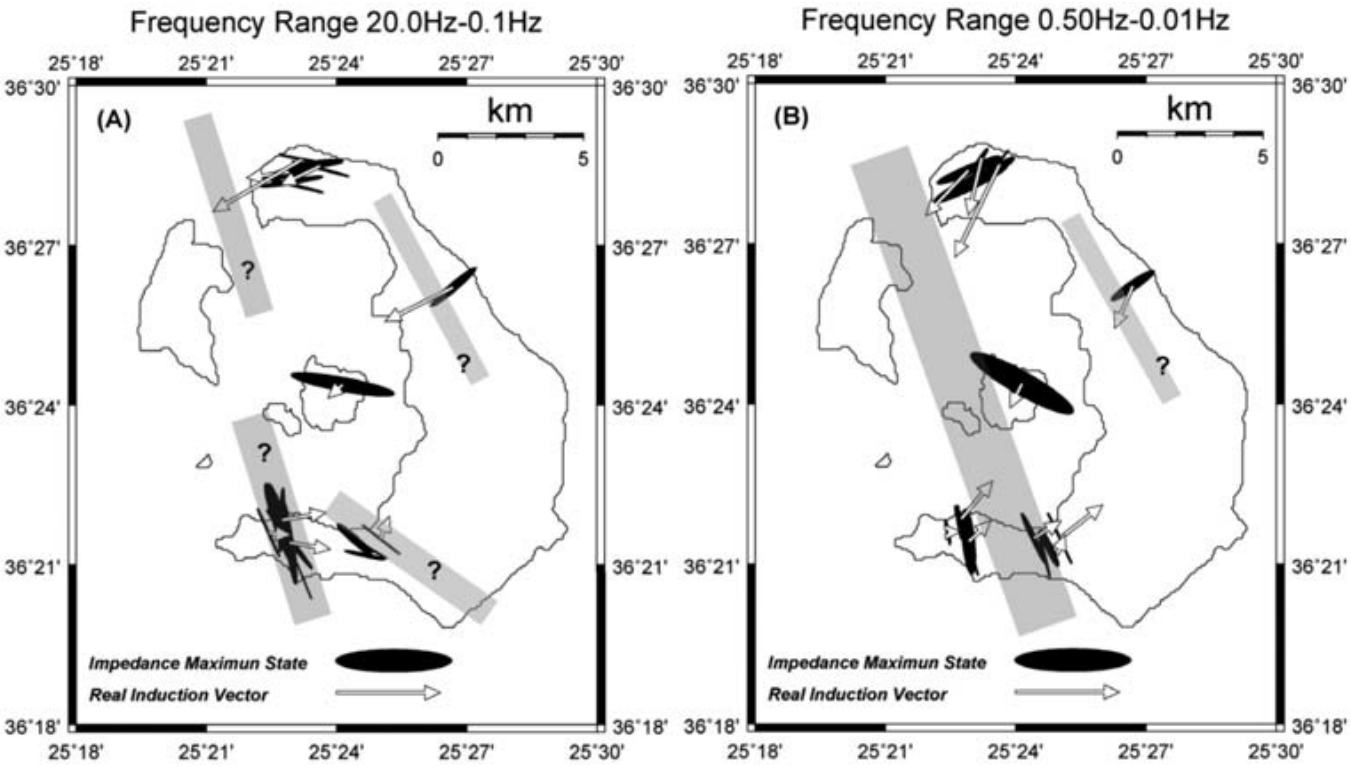

(a) **(b)**

Figure 2. The maximum characteristic states of the electric field (maximum impedance) and the real induction vectors, averaged **(a)** over the band 20 – 1 Hz (*Shallower Structure*), and **(b)** over the band 0.5 – 0.01 Hz (*Deeper Structure*). The thick gray lines represent the approximate location of elongate conductors (after Papageorgiou et al., 2010).

Additional References

Boyce, J.A., Gertisser, R., 2012. Variations in welding characteristics within the Plinian air-fall deposit of the Middle Pumice eruption, Santorini, Greece. J. Volcan. Geothermal Res. 221/222, 71-82.

Budetta, G., Condarelli, D., Fytikas, M., Kolios, N., Pascale, G., Rapolla, A., Pinna, E., 1984. Geophysical prospecting on the Santorini Islands. Bull. Volcanol. 47(3), 447-466.

Fytikas, M., Karydakis, G., Kavouridis, Th., Kolios, N., Vougioukalakis, G., 1989. Geothermal Research on Santorini. In: 'Thera and the Aegean World III', Volume Two: 'Earth Sciences', Proceedings of the Third International Congress. Santorini, Greece, 3-9 September 1989. Publisher: Thera Foundation (1990) ISBN: 0950613371", 241-249.

National Geophysical Data Center (USA), 2012. GEODAS Marine trackline geophysics – Gravity, bathymetry, seismic, geophysical data (Data Banks).

Vassiliadis, K. C., 1985. Geophysical Survey of Thera Island (Santorini) in the frame of the Geothermal Program of IGME. Internal IGME Report (*in Greek*), 10p.

Yokoyama, I., Bonasia, V., 1971. A preliminary gravity survey on Thera Volcano, Greece. Acta, 328-336.

Yokoyama, I. and Bonasia, V., 1979. Gravity anomalies on the Thera Islands. in C. Doumas, (ed.). Thera and the Aegean World-I, 147-150.

2. Comparing GPS and SqueeSAR (Period 1992 – 2010)

GPS and SqueeSAR Velocity Field of SVC Referred to No. 07

	GPS Velocity Field (1994 – 2005)						SqueeSAR Velocity Field (1992 – 2010) Deduced by Combined Ascending & Descending Radar Images					
GPS Station	V_{East} (mm/yr)	σV_{East} (mm/yr)	V_{North} (mm/yr)	σV_{North} (mm/yr)	V_{Up} (mm/yr)	σV_{Up} (mm/yr)	V_{East} (mm/yr)	σV_{East} (mm/yr)	V_{North} (mm/yr)	σV_{North} (mm/yr)	V_{Up} (mm/yr)	σV_{Up} (mm/yr)
02	-1.47	0.55	2.93	0.51	-1.08	1.00	-3.05	0.82	-	-	-1.71	0.37
04	-0.94	0.71	1.95	0.52	1.52	0.61	-2.21	0.31	-	-	0.91	0.25
05	-1.50	0.51	-1.35	0.76	-6.46	0.53	0.26	0.75	-	-	-2.9	0.36
06	-1.32	0.78	0.73	0.81	1.51	0.71	-1.66	0.73	-	-	0.81	0.33
07	-	-	-	-	-	-	-	-	-	-	-	-
12	-1.43	-	-0.33	-	2.01	-	-1.41	0.52	-	-	0.15	0.23
14	-0.46	0.62	-0.12	0.62	2.11	1.12	-0.20	0.61	-	-	0.90	0.34
15	-1.37	0.61	-0.35	0.89	-0.73	0.51	0.24	0.74	-	-	-1.38	0.29
18	-0.41	0.82	0.55	1.10	5.75	1.61	-0.40	0.32	-	-	0.84	0.19
22	-1.14	0.71	-0.91	0.82	-1.69	1.10	-1.16	0.79	-	-	-1.68	0.33
26	-1.93	0.62	0.04	0.71	2.03	1.01	-2.61	0.76	-	-	-0.06	0.18
27	1.11	0.85	-0.36	0.95	5.83	1.10	-0.21	0.71	-	-	0.91	0.34
29	-1.30	0.52	0.52	0.81	2.49	0.80	-0.98	0.62	-	-	0.84	0.29
33	-1.57	0.64	-0.02	0.98	3.38	0.75	-1.96	0.58	-	-	0.48	0.34
43	-0.72	0.54	-0.49	0.81	3.00	0.50	-1.62	0.35	-	-	0.82	0.15
45	-1.01	0.57	-1.78	0.75	-5.48	1.05	0.32	0.72	-	-	-3.26	0.29
56	-0.84	0.51	1.45	0.85	0.88	0.46	-0.73	0.62	-	-	1.19	0.36
57	-0.96	-	1.61	-	0.86	-	-1.21	0.65	-	-	0.74	0.28
99	-0.05	0.81	0.43	0.84	1.02	0.56	-1.09	0.60	-	-	0.89	0.24

σ : velocity errors

3. Strain Field Deduced by GPS Measurements (*Unrest* Period)

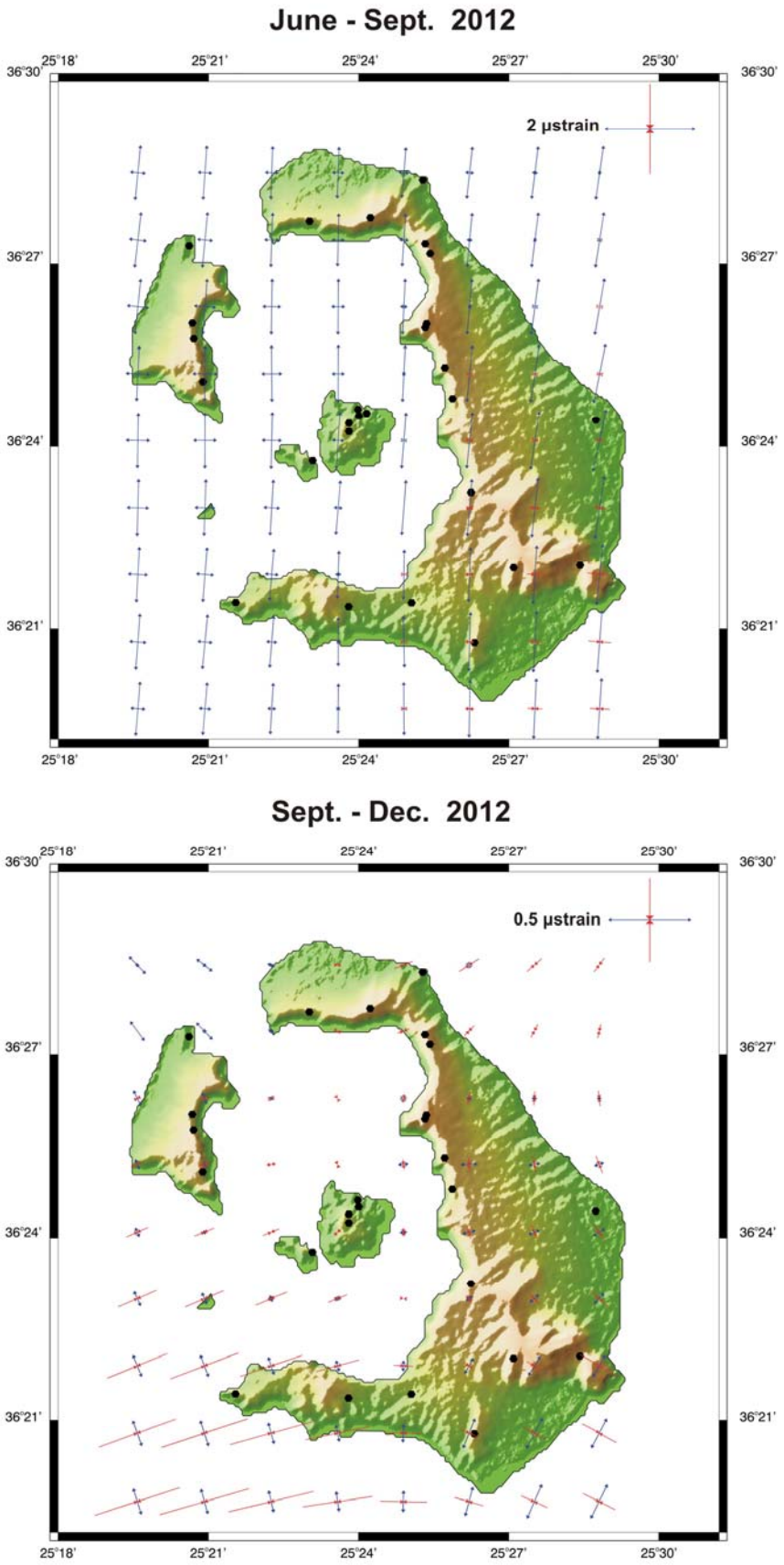

4. Mogi Model Parameter Estimates by various Authors

Author	Mogi Model deduced by GPS				Mogi Model deduced by InSAR (ENVISAT)			
	Period	Location	Depth (km)	Volume ($x10^6$ m^3)	Period	Location	Depth (km)	Volume ($x10^6$ m^3)
Lagios et al. (present paper)	Sept. 2011 to June 2012	25.3888° E 36.4259° N	$4.9^{+0.5}_{-0.5}$	$8.2^{+2.9}_{-1.0}$	Apr. 2011 to Mar. 2012	25.3953° E 36.4262° N	$4.5^{+1.7}_{-0.5}$	$9.2^{+3.2}_{-1.0}$
Newman et al. 2012	Sept. 2011 to Jan. 2012	25.389° E 36.423° N	4.0	9.0	-	-	-	-
Parks et al. 2012	-	-	-	-	March to Dec. 2011	25.389° E 36.430° N	4.4	9.5
Papoutsis et al. 2012	Sept. 2011 to Feb. 2012	25.384° E 36.429° N	$3.5^{+0.19}_{-0.17}$	$12.4^{+0.9}_{-0.8}$	Mar. 2011 to Mar. 2012	25.403° E 36.426° N	$6.3^{+0.02}_{-0.02}$	$24.2^{+0.1}_{-0.1}$

See also "*Santorini_GPS_net.kml*" file

5. Estimated CGPS Velocities for Distinct Periods

	July 2011- Feb. 2012	Feb. – June 2012	June – Nov. 2012	Nov. – Dec. 2012
SANT				
East (mm/yr)	89.8 ± 1.6	59.2 ± 1.7	8.9 ± 1.1	-2.8 ± 5.3
North (mm/yr)	22.1 ± 0.8	4.1 ± 1.0	-18.9 ± 0.8	-0.9 ± 5.2
Up (mm/yr)	58.2 ± 2.2	29.4 ± 3.9	3.4 ± 2.6	16.5 ± 14.4
RIBA				
East (mm/yr)	-67.1 ± 1.5	-22.8 ± 1.2	2.3 ± 0.7	11.4 ±6.3
North (mm/yr)	36.2 ± 1.4	4.7 ± 1.0	-17.0 ± 0.9	-10.3±9.8
Up (mm/yr)	61.1 ± 4.7	1.4 ± 3.8	-0.2 ± 2.5	26.5±31.7
KERA				
East (mm/yr)	-77.1 ± 1.5	-40.9 ± 1.6	-2.4 ± 1.0	8.3 ± 5.0
North (mm/yr)	-20.9 ± 0.7	-22.2 ± 1.1	-16.8 ± 0.8	-4.0 ± 4.5
Up (mm/yr)	57.9 ± 2.6	22.5 ± 3.9	-2.0 ± 2.3	7.1 ± 16.4
PKMN				
East (mm/yr)	-7.4 ± 0.9	1.7 ± 0.9	1.2 ± 0.7	8.3 ± 4.1
North (mm/yr)	-77.1 ± 1.1	-55.8 ± 1.3	-23.4 ± 0.9	-0.2 ± 4.8
Up (mm/yr)	64.0 ± 3.1	20.1 ± 3.6	0.9 ± 2.8	37.4 ± 13.4
NOMI				
East (mm/yr)	79.6 ± 0.9	58.1 ± 1.6	10.5 ± 0.9	11.5 ± 5.6
North (mm/yr)	-13.8 ± 0.5	-15.6 ± 1.1	-19.6 ± 0.9	-0.7 ± 5.1
Up (mm/yr)	57.3 ± 1.6	27.6 ± 3.7	6.5 ± 2.5	23.5 ± 15.7
MOZI				
East (mm/yr)	71.6 ± 2.4	41.0 ± 1.9	6.6 ± 0.7	4.4 ± 4.5
North (mm/yr)	55.3 ± 1.7	21.1 ± 1.1	-15.3 ± 1.1	-4.8 ± 4.7
Up (mm/yr)	64.4 ± 5.0	16.6 ± 3.8	4.6 ± 2.3	9.7 ± 13.4
MKMN				
East (mm/yr)	-	29.6 ± 1.3	8.5 ± 1.4	-
North (mm/yr)	-	-50.7 ± 1.4	-25.5 ± 1.3	-
Up (mm/yr)	-	24.1 ± 3.9	1.0 ± 5.3	-

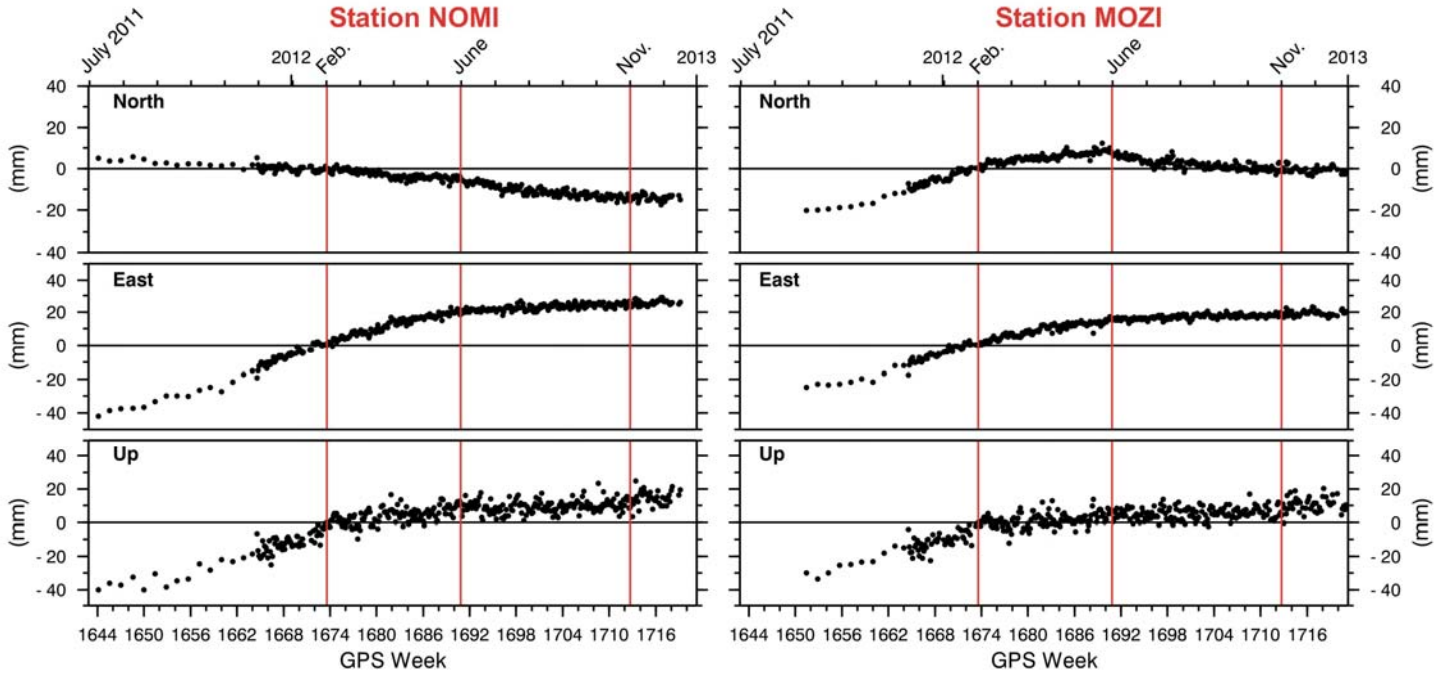
Station NOMI
July 2011
2012
Feb.
June
Nov.
2013
North
East
Up
(mm)
40
20
0
- 20
- 40
1644 1650 1656 1662 1668 1674 1680 1686 1692 1698 1704 1710 1716
GPS Week

Station MOZI
July 2011
2012
Feb.
June
Nov.
2013
North
East
Up
(mm)
40
20
0
- 20
- 40
1644 1650 1656 1662 1668 1674 1680 1686 1692 1698 1704 1710 1716
GPS Week

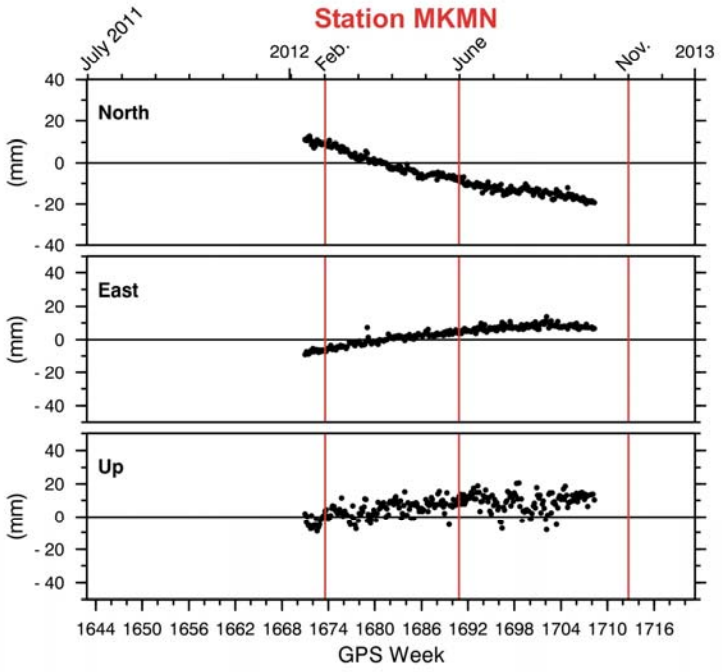
Station MKMN
July 2011
2012
Feb.
June
Nov.
2013
North
East
Up
(mm)
40
20
0
- 20
- 40
1644 1650 1656 1662 1668 1674 1680 1686 1692 1698 1704 1710 1716
GPS Week

6. PS/DS Time Series for selected points in Nea Kammeni & Therassia for the Period 1992-2010

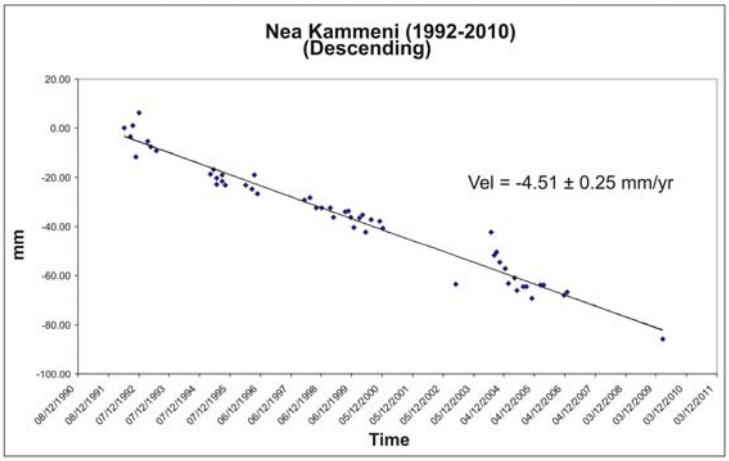

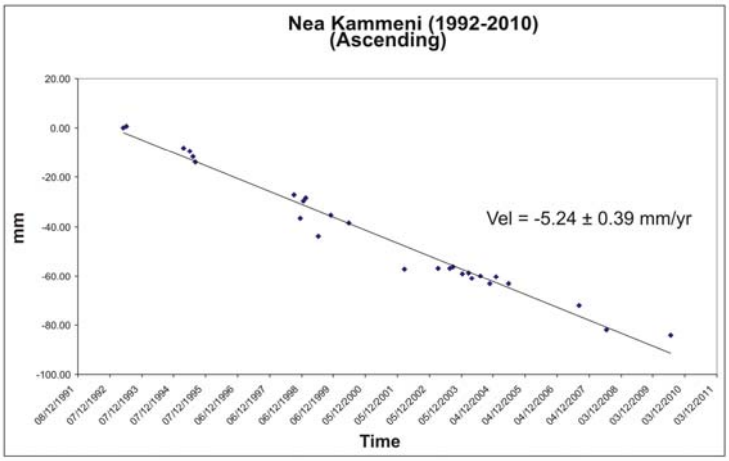

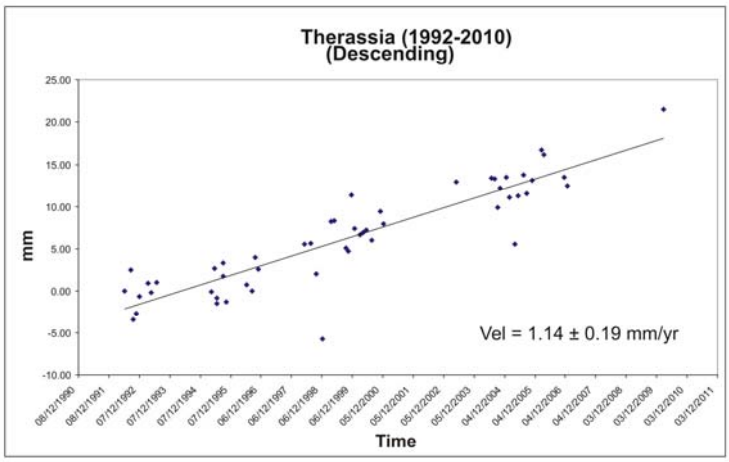

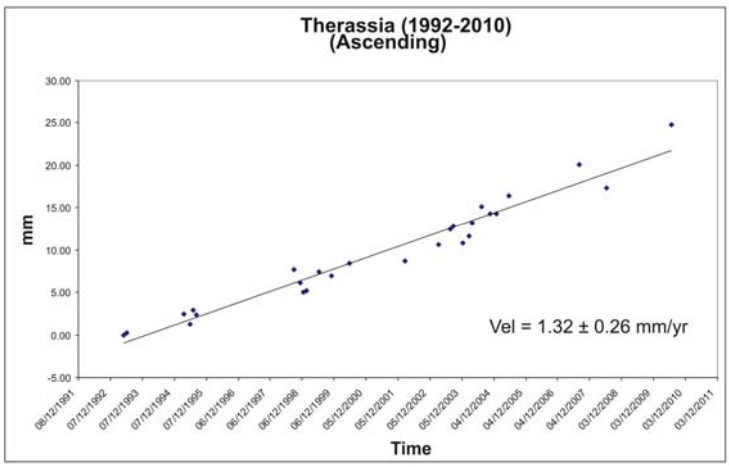

7. PS/DS Time Series for selected points in Kammenis & Imerovigli for the Period 2011-2012